

Lyapunov exponents of the Kuramoto–Sivashinsky PDE

Russell A. Edson ^{*} J. E. Bunder [†] Trent W. Mattner [‡]
 A. J. Roberts [§]

2019-02-27

Abstract

The Kuramoto–Sivashinsky equation is a prototypical chaotic non-linear partial differential equation (PDE) in which the size of the spatial domain plays the role of a bifurcation parameter. We investigate the changing dynamics of the Kuramoto–Sivashinsky PDE by calculating the Lyapunov spectra over a large range of domain sizes. Our comprehensive computation and analysis of the Lyapunov exponents and the associated Kaplan–Yorke dimension provides new insights into the chaotic dynamics of the Kuramoto–Sivashinsky PDE, and the transition to its 1D turbulence.

Contents

1	Introduction	2
2	The Kuramoto–Sivashinsky equation	3
3	Evaluate the Lyapunov exponents	7

^{*}School of Mathematical Sciences, University of Adelaide, South Australia. <mailto:russell.edson@adelaide.edu.au> , <https://orcid.org/0000-0002-4607-5396>

[†]School of Mathematical Sciences, University of Adelaide, South Australia. <mailto:judith.bunder@adelaide.edu.au> , <http://orcid.org/0000-0001-5355-2288>

[‡]School of Mathematical Sciences, University of Adelaide, South Australia. <mailto:trent.mattner@adelaide.edu.au> , <https://orcid.org/0000-0002-5313-5887>

[§]School of Mathematical Sciences, University of Adelaide, South Australia. <mailto:anthony.roberts@adelaide.edu.au> , <http://orcid.org/0000-0001-8930-1552>

<i>1 Introduction</i>	2
4 Compute the Kaplan–Yorke dimension	14
5 Conclusion	17

1 Introduction

The Kuramoto–Sivashinsky PDE (1) models a wide variety of nonlinear systems with intrinsic instabilities, such as wave propagation in chemical reaction-diffusion systems (Kuramoto and Tsuzuki 1976), the velocity of laminar flame front instabilities (Sivashinsky 1977), thin fluid film flow down inclined planes (Sivashinsky and Michelson 1980), and hydrodynamic turbulence (e.g., Pomeau and Zaleski 1985; Hohenberg and Sraiman 1989; Dankowicz et al. 1996). In the Kuramoto–Sivashinsky PDE the large scale dynamics are dominated by a destabilising ‘diffusion’, whereas small scale dynamics are dominated by stabilising hyperdiffusion, and a nonlinear advective term stabilises the system by transferring energy from the large unstable modes to the small stable modes (e.g., Sprott 2010, p. 199). The interplay between these contrasting features leads to significant spatio-temporal complexity (e.g., Hyman and Nicolaenko 1986; Cross and Hohenberg 1993; Cvitanović, Davidchack, and Siminos 2010), from intermittent disorder, through to chaos, hyperchaos and turbulence. Lyapunov exponents characterise this chaos and turbulence (e.g., Eckmann and Ruelle 1985; Ruelle and Takens 1971; Takens 1981), and are increasingly used to analyse such spatio-temporal complexity in various applications such as turbulent Poiseuille flow (Keefe, Moin, and Kim 1992), turbulence in flames (Hassanally and Raman 2018), and Rayleigh–Bérnard fluid convection (Chertovskih, Chimanski, and Rempel 2015; Xu 2017).

Here we show new details of how the dynamics of the Kuramoto–Sivashinsky PDE become increasingly chaotic as the size of the domain increases, for both periodic and odd-periodic boundary conditions. To measure the degree of chaos, Section 3 computes the Lyapunov exponents using the classic algorithm introduced by Benettin et al. (1980a) and Shimada and Nagashima (1979), but now in new detail over a comprehensive range of domain sizes. By comparison, Tajima and Greenside (2002) explored the Kuramoto–Sivashinsky PDE (1) with rigid boundary conditions over a range of domain lengths, whereas we explore periodic (2) and odd-periodic (3) cases, we use an order of magnitude increased resolution in the domain lengths, and we also cover the transition to chaos regime. The Lyapunov exponents describe the rate at which neighbouring trajectories diverge under a chaotic flow, and thus

provide a quantitative measure of the degree of chaos in a system. Section 3 analyses the growth of the Lyapunov exponents with increasing domain size, and then uses the Lyapunov spectra to identify the onset of chaos and to characterise new details of the increasingly complex spatio-temporal dynamics of the Kuramoto–Sivashinsky PDE.

A further use of the Lyapunov exponents is in defining the Kaplan–Yorke dimension of the attractor of a dynamical system (Kaplan and Yorke 1979). The Kaplan–Yorke dimension bounds above the fractal dimension of the chaotic attractor, and approximates the number of effective modes necessary to describe the dynamics on the attractor (Grassberger and Procaccia 1983). For a Kuramoto–Sivashinsky PDE defined on either a periodic or odd-periodic domain, Section 4 confirms more accurately how the Kaplan–Yorke dimension scales roughly linearly with the domain size. This linear scaling corresponds well with the scaling observed by Manneville (1985) and Tajima and Greenside (2002) for the Kuramoto–Sivashinsky PDE with rigid boundary conditions.

Our detailed analysis of the chaotic dynamics of the Kuramoto–Sivashinsky PDE and its dependence on domain size provides new insights into the onset of chaos. In many chaotic systems, we can identify that discrete point at which a bifurcation parameter permits chaos, but our new visualisation of the comprehensive computation of Lyapunov exponents highlights the gradual changes which drive a system into the chaotic regime, and thence into 1D turbulence.

2 The Kuramoto–Sivashinsky equation

On the spatial domain $0 \leq x \leq L$ for some domain size L , the one-dimensional Kuramoto–Sivashinsky PDE for field $u(x, t)$ is

$$\partial_t u + \partial_x^4 u + \partial_x^2 u + u \partial_x u = 0. \quad (1)$$

We apply either periodic boundary conditions,

$$u(x + L, t) = u(x, t) \quad \text{for all } 0 \leq x \leq L, \quad (2)$$

or odd-periodic boundary conditions,

$$u(x, t) = \partial_x^2 u(x, t) = 0 \quad \text{at } x = 0, L. \quad (3)$$

In the Kuramoto–Sivashinsky PDE, the second order diffusive term $\partial_x^2 u$ is destabilising whereas the fourth order hyperdiffusion term $\partial_x^4 u$ is stabilising,

resulting in large scale instabilities and small scale dissipation, with the transfer of energy from large to small scales, mediated by the nonlinear term $\mathbf{u}\partial_x\mathbf{u}$, producing a stabilising influence on the system (e.g., Sprott 2010, p. 199).

The Kuramoto–Sivashinsky PDE (1) supports several symmetries, although in the turbulent regime they only hold in a time-averaged sense (e.g., Wittenberg and Holmes 1999; Cvitanović, Davidchack, and Siminos 2010). Of particular interest for periodic domains (2) are the Galilean invariance, $\mathbf{u}(\mathbf{x}, t) \rightarrow \mathbf{u}(\mathbf{x} - \mathbf{c}t, t) + \mathbf{c}$ for all speeds \mathbf{c} , and the spatial translation invariance, $\mathbf{u}(\mathbf{x}, t) \rightarrow \mathbf{u}(\mathbf{x} + \mathbf{d}, t)$ for all \mathbf{d} . These two symmetries do not hold for odd-periodic domains (3). The Kuramoto–Sivashinsky PDE (1) with odd-periodic domains (3) is particularly well studied (e.g., Rempel et al. 2004; Lan and Cvitanović 2008; Foias et al. 1986; Eguíluz et al. 1999) compared to that with periodic domains, as the removal of periodic symmetries simplifies somewhat the analysis of the dynamics. The relatively simpler dynamics of the odd-periodic case is observed in Section 3 when comparing the periodic and odd-periodic Lyapunov spectra. The most obvious point of difference is that the Galilean and translation invariances support two zero Lyapunov exponents which are absent from the Lyapunov spectra for the odd-periodic case. Commonly for the periodic case, a zero mean condition is imposed to remove the Galilean invariance and consequently one of the zero Lyapunov exponents (e.g., Cvitanović, Davidchack, and Siminos 2010; Wittenberg and Holmes 1999; Dankowicz et al. 1996); we do not impose the zero mean condition.

As the size L of the spatial domain varies, the Kuramoto–Sivashinsky PDE (1) produces distinctly different dynamics (e.g., Hyman and Nicolaenko 1986; Cross and Hohenberg 1993; Cvitanović, Davidchack, and Siminos 2010). For periodic boundary conditions (2), Figure 1 shows the increasing complexity of the Kuramoto–Sivashinsky dynamics as domain size L increases, from stable travelling wave when $L \lesssim 13$ through to a spatio-temporal chaotic turbulence when $L \approx 100$. Figure 2 for odd-periodic boundary conditions (3) also shows an increase in the complexity of the dynamics as L increases, progressing from an oscillating cell when $L \lesssim 17$ through to a spatio-temporal turbulence when $L \approx 100$. For both types of boundary conditions, the spatial domain size L plays the role of a bifurcation parameter.

Our aim is to provide new details of the character of the trend to spatio-temporal complexity and ‘turbulence’ with increasingly long domains L . To do this, Section 3 comprehensively computes the 24 most positive Lyapunov exponents across a significant range of domain lengths L . It is these ‘most

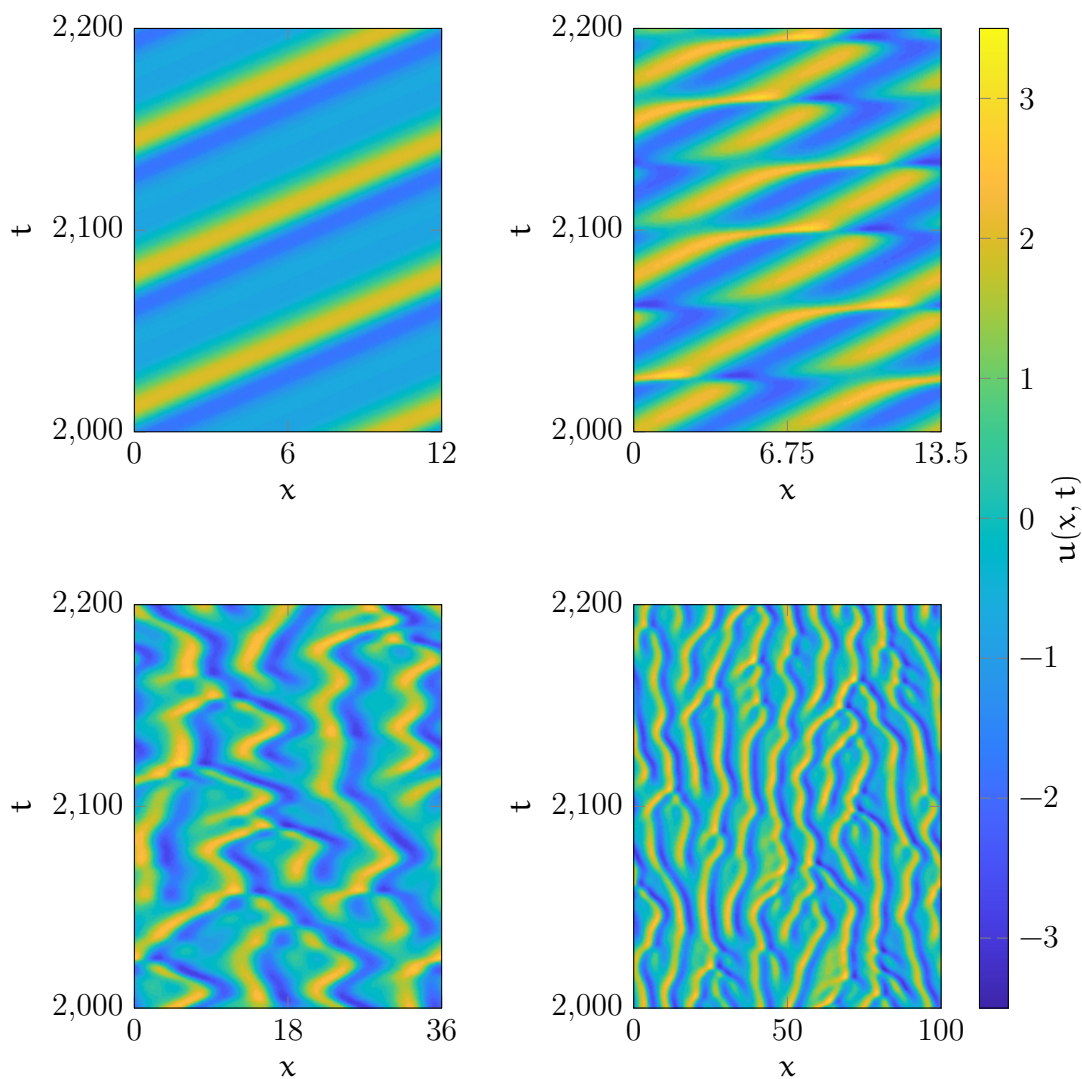


Figure 1: Simulations of the Kuramoto–Sivashinsky PDE (1)+(2) depend upon the size of the periodic spatial domain L : (top left) for $L = 12$, a travelling wave emerges; (top right) for $L = 13.5$, intermittent bursts disrupt the travelling wave structure; (bottom left) for $L = 36$, chaotic cellular structures criss-cross and interact; and (bottom right) for $L = 100$, spatio-temporally complex patterns of ‘turbulence’.

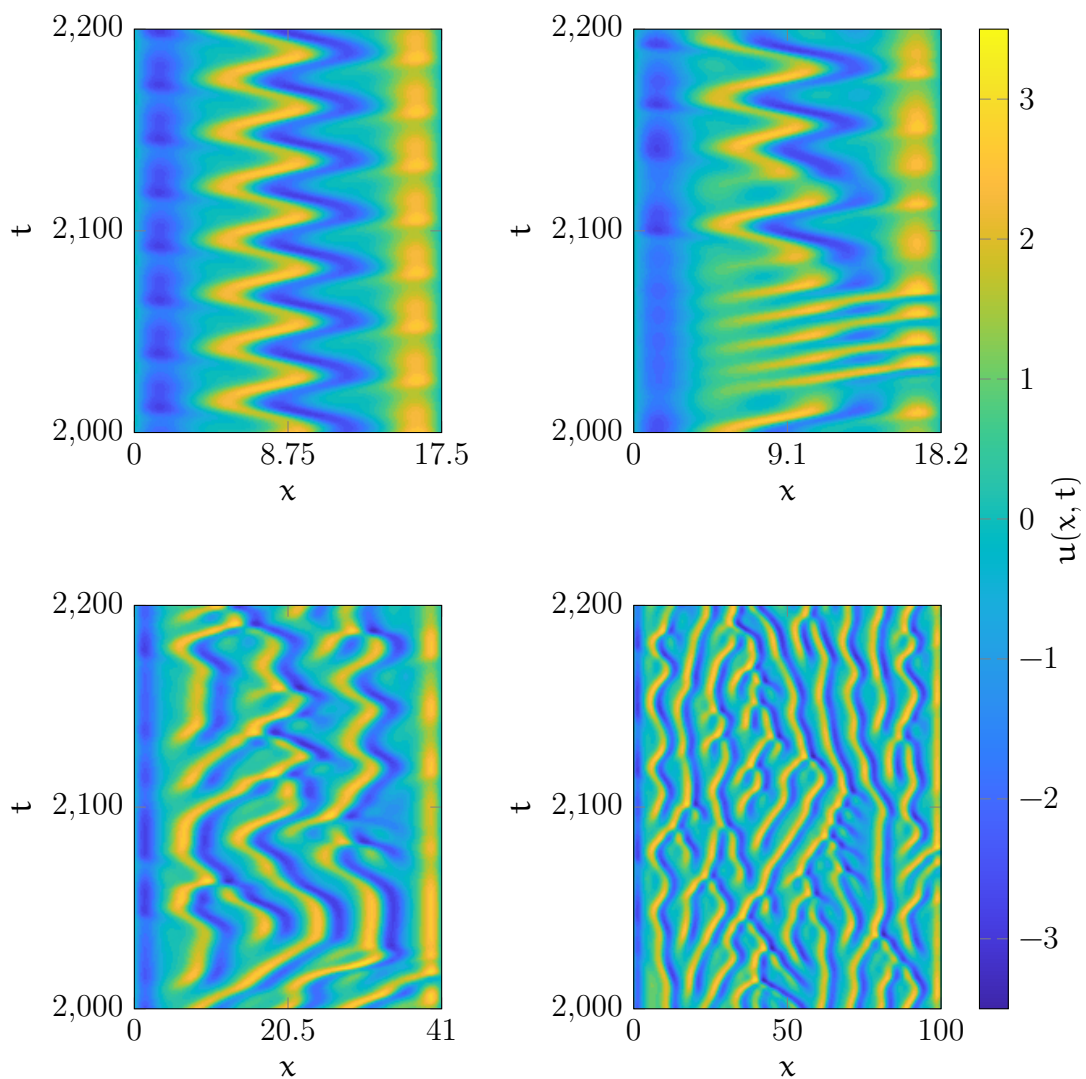


Figure 2: Simulations of the Kuramoto–Sivashinsky PDE (1)+(3) depend upon the size of the odd-periodic spatial domain L : (top left) for $L = 17.5$, an oscillating cell emerges; (top right) for $L = 18.2$, intermittent bursts disrupt the cell structure; (bottom left) for $L = 41$, chaotic cellular structures criss-cross and interact; and (bottom right) for $L = 100$, spatio-temporally complex patterns of ‘turbulence’.

positive' Lyapunov exponents which determine the nature of the chaotic dynamics. Then, Section 4 evaluates the Kaplan–Yorke dimension over the same range of L to show more information about how the dimension of the chaotic attractor grows linearly with L .

3 Evaluate the Lyapunov exponents

In a dynamical system, the Lyapunov exponents measure the exponential divergence of initially close trajectories, with positive Lyapunov exponents indicating divergent trajectories and negative Lyapunov exponents indicating convergence (Chicone 2006; Eckmann and Ruelle 1985). A chaotic system, due to its sensitivity to initial conditions, must have at least one positive Lyapunov exponent. Furthermore, an increasingly chaotic system has an increasing number of positive Lyapunov exponents. This section evaluates Lyapunov exponents of the Kuramoto–Sivashinsky PDE (1) for increasing domain size L and interprets each increase in the number of positive Lyapunov exponents as a transition to an increasingly chaotic system.

Formally, Lyapunov exponents measure trajectory divergences in the infinite time limit, with different Lyapunov exponents corresponding to divergences in different orthogonal directions. The existence of these time limits are assured (almost everywhere) by Oseledec's multiplicative ergodic theorem (e.g., Eckmann and Ruelle 1985; Ruelle 1979). In numerical calculations of Lyapunov exponents, complications due to the infinite time limit are avoided by computing N iterations of the divergence of trajectories over finite time intervals T , with N large but finite (e.g., Shimada and Nagashima 1979; Benettin et al. 1980b; Geist, Parlitz, and Lauterborn 1990; Dieci, Russell, and Van Vleck 1997; Skokos 2010). At the end of each iteration, the divergent trajectories are reorthonormalised. This reorthonormalisation ensures the tracked directions remain orthogonal, rather than all converging to that of the largest positive Lyapunov exponent (e.g., Geist, Parlitz, and Lauterborn 1990). This rescaling is valid in the ergodic case because the Lyapunov exponents are (almost everywhere) independent of a trajectory's initial condition. However, the finite time numerical approximation generally results in some numerical error (e.g., Dieci, Russell, and Van Vleck 1997).

Algorithm 1 assumes a vector function of time, $\mathbf{u}(\mathbf{t}) \in \mathbb{R}^n$, satisfies the dynamical system

$$\dot{\mathbf{u}} = \mathbf{f}(\mathbf{t}, \mathbf{u}), \quad (4)$$

with initial condition $\mathbf{u}(0)$. Trajectories are first evolved for time τ to ensure

initial transients have decayed and thus that the system is close to an attractor. Then Algorithm 1 numerically solves the ODE (4) for a time $N \cdot T$ to compute the m most positive Lyapunov exponents λ_i for $i = 1, \dots, m \leq n$ using reduced QR decomposition to reorthonormalise after each of N time intervals of length T (e.g., Shimada and Nagashima 1979; Benettin et al. 1980b; Geist, Parlitz, and Lauterborn 1990; Dieci, Russell, and Van Vleck 1997; Skokos 2010). As is standard, the resulting Lyapunov exponents are ordered such that $\lambda_1 \geq \lambda_2 \geq \dots \geq \lambda_m$.

Algorithm 1 The classic algorithm for computing the spectrum of Lyapunov exponents for a dynamical system, introduced by Benettin et al. (1980a), and Shimada and Nagashima (1979).

$\mathbf{du}/dt = \mathbf{f}(t, \mathbf{u})$: the dynamical system ODE

$\mathbf{u}(0)$: the initial value of \mathbf{u}

m : the number of the most positive exponents to compute

τ : time to simulate system before computing exponents

T : time between reorthonormalisation steps

N : the total number of reorthonormalisation steps

ϵ : perturbation magnitude (typically take $\epsilon = 10^{-6}$).

OUTPUT:

λ_i : the m most positive Lyapunov exponents, $i = 1, \dots, m$.

- 1: compute $\mathbf{u}^{(0)} := \mathbf{u}(\tau)$ via solving ODE on $[0, \tau]$
 - 2: set $t_j := \tau + jT$, for $j = 0, 1, 2, \dots, N$
 - 3: choose initial orthogonal directions $\mathbf{Q}^{(0)} := \begin{bmatrix} \mathbf{q}_1^{(0)} & \dots & \mathbf{q}_m^{(0)} \end{bmatrix}$
 - 4: **for** $j = 1 : N$ **do**
 - 5: compute $\mathbf{u}^{(j)} := \mathbf{u}(t_j)$ via solving ODE with $\mathbf{u}(t_{j-1}) = \mathbf{u}^{(j-1)}$
 - 6: **for** $i = 1 : m$ **do**
 - 7: compute $\mathbf{w}_i^{(j)} := \mathbf{u}(t_j)$ via ODE with $\mathbf{u}(t_{j-1}) = \mathbf{u}^{(j-1)} + \epsilon \mathbf{q}_i^{(j-1)}$
 - 8: approximate $\Psi(t_j, t_{j-1}) \mathbf{q}_i^{(j-1)} := (\mathbf{w}_i^{(j)} - \mathbf{u}^{(j)})/\epsilon$
 - 9: **end for**
 - 10: construct $\Psi(t_j, t_{j-1}) \mathbf{Q}^{(j-1)} := \begin{bmatrix} \Psi(t_j, t_{j-1}) \mathbf{q}_1^{(j-1)} & \dots & \Psi(t_j, t_{j-1}) \mathbf{q}_m^{(j-1)} \end{bmatrix}$
 - 11: compute $\mathbf{Q}^{(j)} \mathbf{R}^{(j)} := \text{QR}(\Psi(t_j, t_{j-1}) \mathbf{Q}^{(j-1)})$
 - 12: **end for**
 - 13: **for** $i = 1 : m$ **do**
 - 14: compute $\lambda_i := \sum_{j=1}^N \log R_{i,i}^{(j)} / (NT)$
 - 15: **end for**
 - 16: **return** $\{\lambda_i\}$.
-

In implementing Algorithm 1 for the Kuramoto–Sivashinsky PDE (1) a n -

D approximate system is used, either spectral in space for the periodic case (2) or finite differences for the odd-periodic case (3). In either case we choose truncations so that the maximum wavenumber resolved was $k_{\max} \approx 9$ (which decays extremely rapidly, on a time scale of $1/k_{\max}^4 \approx 10^{-4}$). Initial conditions were random and normally distributed $\sim \mathcal{N}(0, 1)$. After some testing of different transient times τ , we selected $\tau = 2000$, which is smaller than some other studies (e.g., Wittenberg and Holmes (1999) used $\tau = 100\,000$), but repeatedly provided consistent and expected dynamics. A total of $N = 1000$ reorthonormalisation steps are performed in the exponent computations. This choice of N computes fairly accurate Lyapunov exponents within a reasonable time frame.

An important decision in the numerical calculation of the Lyapunov spectrum is the size of each time interval T between reorthonormalisations. Figure 3 demonstrates how the choice of interval T in Algorithm 1 affects the calculation of the $m = 24$ most positive Lyapunov exponents, for small domain $L = 20$ or large domain $L = 100$, in the case of odd-periodic boundary conditions (3) (the periodic case (2) provides similar plots). For small interval T ($T \lesssim 0.1$ for $L = 20$, and $T \lesssim 1$ for $L = 100$) the most positive Lyapunov exponents are inaccurate because T is too small to sufficiently capture the trajectory divergence, leading to an unstable QR decomposition. For larger interval T ($T \gtrsim 0.1$ for $L = 20$, and $T \gtrsim 10$ for $L = 100$) the most negative of the $m = 24$ Lyapunov exponents evolve for too long and are corrupted towards the more positive exponents. Based upon Figure 3 we generally chose reorthonormalisation interval $T = 2$. With this choice of T we accurately resolve the most positive Lyapunov exponents, while also computing a sufficient number of negative Lyapunov exponents for the evaluation of the Kaplan–Yorke dimension for the chosen range of domains.

Figures 4 and 5 plot the 24 most positive Lyapunov exponents for the Kuramoto–Sivashinsky PDE (1) over different domain sizes, $0 < L \leq 100$ with periodic (2) and odd-periodic (3) boundary conditions, respectively. Although these calculations of the Lyapunov exponents contain noise, the exponents generally increase as L increases, and larger values of L generally have more positive exponents. However, the increase in the Lyapunov exponents is limited as they appear to be bounded above by about 0.1, for both the periodic and odd-periodic cases. This upper bound 0.1 matches with the upper bound observed for the rigid boundary condition case (Yang et al. 2009; Manneville 1985).

We now further explore the Lyapunov exponents in the periodic case. The structure of the positive Lyapunov exponents is noisy but there are some

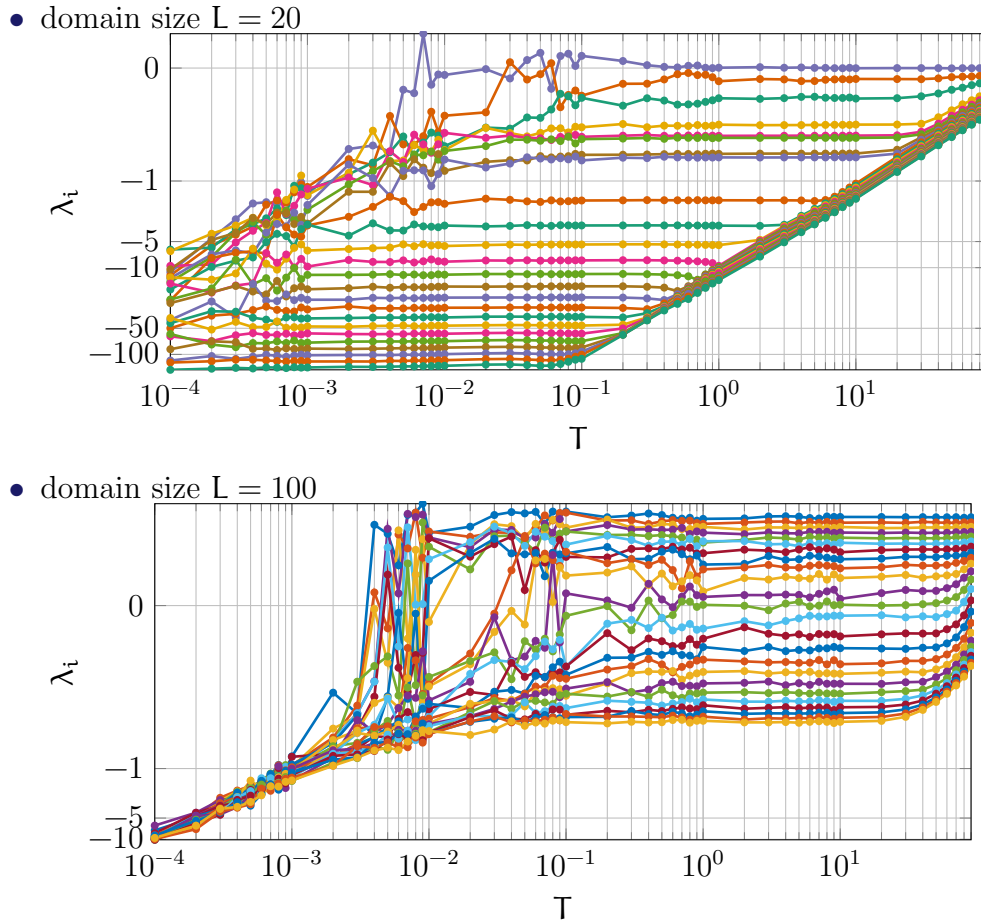


Figure 3: The $m = 24$ most positive Lyapunov exponents λ_i for (top) $L = 20$ and (bottom) $L = 100$ calculated using Algorithm 1 with odd-periodic boundary conditions (3) and different interval times T . An accurate Lyapunov exponent is approximately constant as T varies. When $L = 20$ there is no range of T for which *all* 24 exponents are constant, but the most negative ones are least important. For $L = 100$, all $m = 24$ Lyapunov exponents are reasonably constant for $1 < T < 10$.

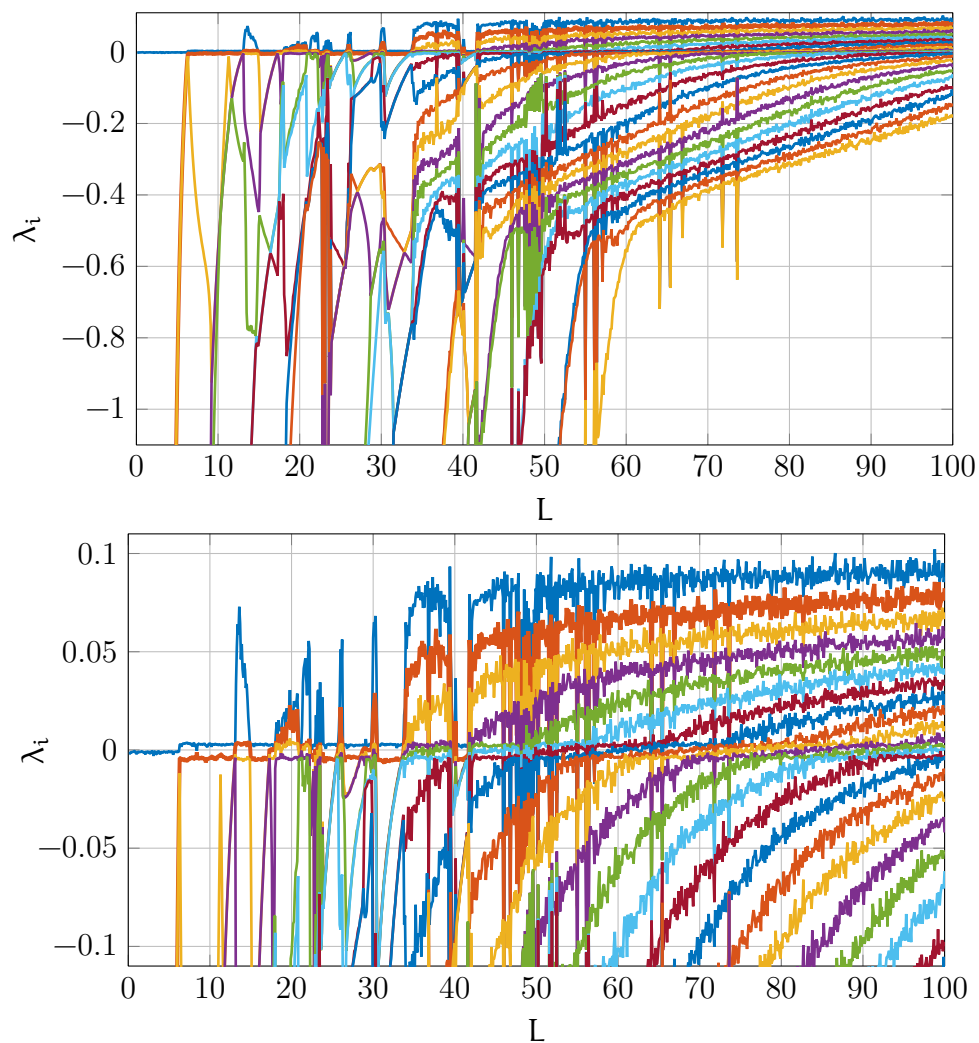


Figure 4: The 24 most positive Lyapunov exponents $\lambda_1, \lambda_2, \dots, \lambda_{24}$, computed for the Kuramoto–Sivashinsky PDE (1) on the periodic (2) spatial domain for domain sizes $0 < L \leq 100$. The bottom plot zooms into those Lyapunov exponents near zero.

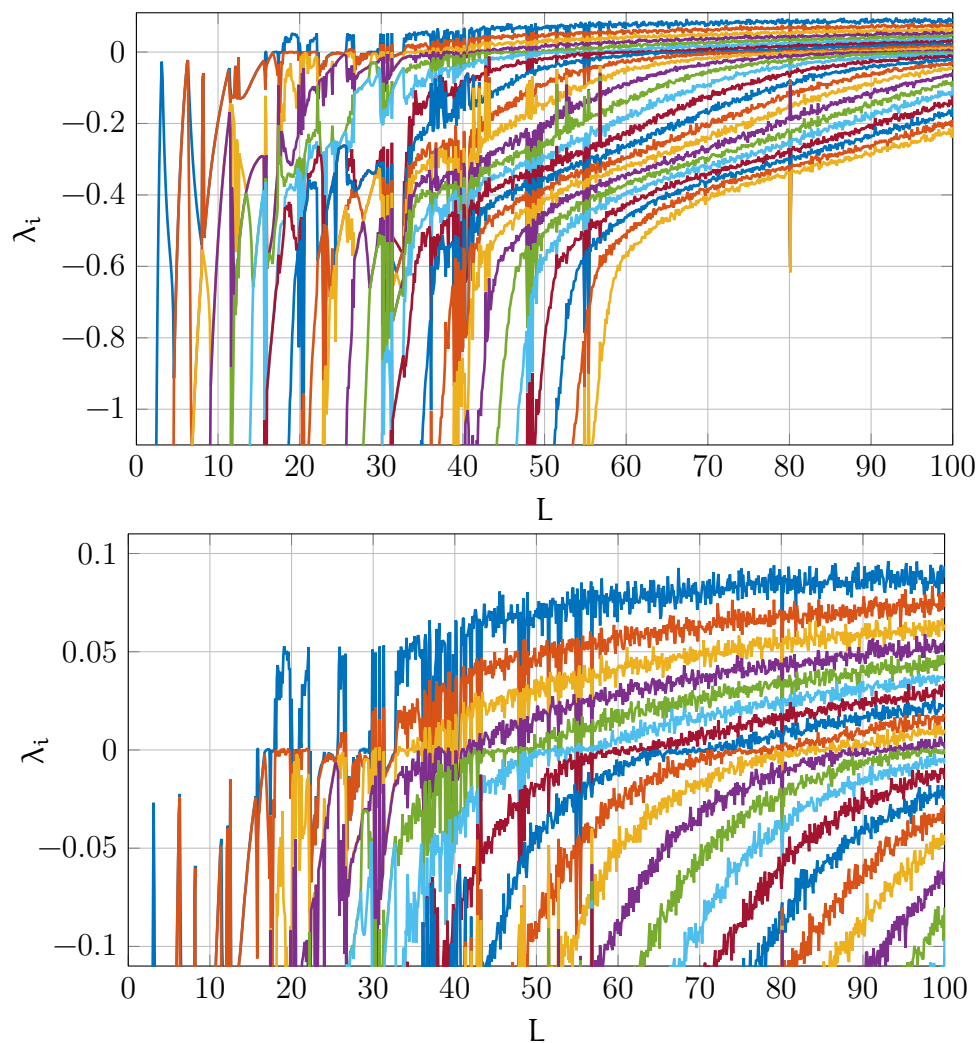


Figure 5: The 24 most positive Lyapunov exponents $\lambda_1, \lambda_2, \dots, \lambda_{24}$, computed for the Kuramoto–Sivashinsky PDE (1) on the odd-periodic (3) spatial domain for domain sizes $0 < L \leq 100$. The bottom plot provides a more detailed look at those Lyapunov exponents near zero.

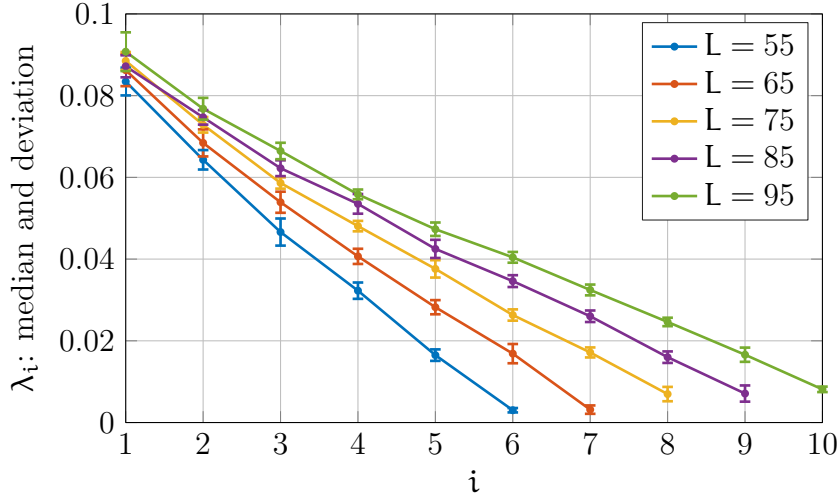


Figure 6: Positive Lyapunov exponents λ_i for the periodic case (2), Figure 4, as a function of index i . The joining lines are purely to aid visualisation. The data points plotted for each L are the medians over the window $[L - 1, L + 1]$, \pm -the mean absolute deviation.

reasonably clear trends: here we show that the i th positive Lyapunov exponent on a domain length L is approximately

$$\lambda_i(L) \approx 0.093 - 0.94(i - 0.39)/L. \quad (5)$$

To derive this approximation, first look at the i -dependence for various fixed L : Figure 6 plots Lyapunov exponents $\lambda_i(L)$ for fixed L as a function of index i . Since the data from Figure 4 is noisy, the median of the Lyapunov exponent is plotted where the median is over the window $[L - 1, L + 1]$ (21 data points). Then the vertical bars for each point represent plus-and-minus the mean absolute deviation (MAD): these statistics are more robust to outliers than the usual mean and standard deviation, and so appear more suitable here. Figure 6 indicates the Lyapunov exponents are, for fixed L , approximately equi-spaced in i , especially for $i \leq 5$. The magnitude of the slope of the i -dependence decreases as the domain length L increases, so we try to fit a function of the power-law form $\lambda_i(L) \approx a + (b + ci)/L^p$ for various exponents p . Figure 7 plots the residual error in the fit as a function of exponent p showing that there is a minimum error at $p \approx 1$: this minimum occurs both in the RMS error and the MAD error. In view of the fluctuations in the MAD, it seems reasonable to choose the case of the exponent $p = 1$ reported by equation (5). Moreover, this is the exponent which best fits our preconception that the chaos in the Kuramoto–Sivashinsky PDE is ‘extensive’—that the number of

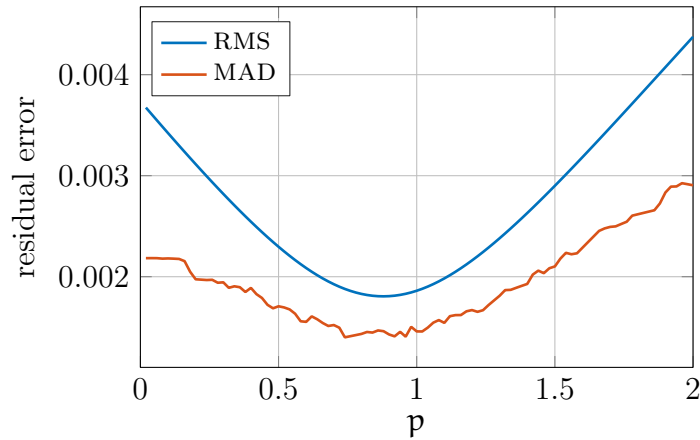


Figure 7: Fit the Lyapunov exponents $\lambda_i(L) \approx \mathbf{a} + (\mathbf{b} + \mathbf{c}i)/L^p$ for various exponents p and then plot the residual error as a function of exponent p : here the root-mean-square error (RMS), and the mean absolute deviation (MAD). The minimum suggests the optimum exponent $p \approx 1$.

positive Lyapunov exponents increases linearly with domain length L . The next Section 4 explores this issue further via the Kaplan–Yorke dimension, and finds results consistent with the approximate formula (5).

4 Compute the Kaplan–Yorke dimension

The Kaplan–Yorke dimension is a measure of the dimension of an attractor (Kaplan and Yorke 1979) and is defined in terms of a sum of the most positive Lyapunov exponents,

$$D_{KY} = j + \frac{\sum_{i=1}^j \lambda_i}{|\lambda_{j+1}|}, \quad (6)$$

where j is the largest index such that $\sum_{i=1}^j \lambda_i \geq 0$. The Kaplan–Yorke dimension is an upper bound of the Hausdorff dimension of the attractor, and as each of the j Lyapunov exponents correspond to an orthogonal direction, the Kaplan–Yorke dimension approximates the minimum number of modes required to describe the emergent dynamics of the system on the attractor (Grassberger and Procaccia 1983).

In the formula (6) the term $\sum_{i=1}^j \lambda_i / |\lambda_{j+1}|$ is usually a fraction in $(0, 1)$ and so the index j is roughly the Kaplan–Yorke dimension. Using the approximation (5) to the Lyapunov exponents for the periodic case, one may

Table 1: the 12 most positive Lyapunov exponents and the Kaplan–Yorke dimension for several domain sizes L and periodic boundary conditions (2).

	$L = 12$	$L = 13.5$	$L = 22$	$L = 36$	$L = 60$	$L = 100$
λ_1	0.003	0.059	0.043	0.080	0.089	0.088
λ_2	-0.005	0.004	0.003	0.056	0.067	0.082
λ_3	-0.088	-0.004	0.002	0.014	0.055	0.070
λ_4	-0.089	-0.227	-0.004	0.003	0.041	0.061
λ_5	-0.186	-0.730	-0.008	-0.003	0.030	0.048
λ_6	-3.524	-1.467	-0.185	-0.004	0.005	0.041
λ_7	-3.525	-1.529	-0.253	-0.021	0.003	0.033
λ_8	-9.835	-6.956	-0.296	-0.088	0.000	0.028
λ_9	-9.849	-6.963	-0.309	-0.160	-0.004	0.018
λ_{10}	-9.959	-7.977	-1.965	-0.224	-0.009	0.012
λ_{11}	-10.01	-7.993	-1.967	-0.309	-0.029	0.005
λ_{12}	-10.12	-9.199	-5.599	-0.373	-0.066	0.003
D_{KY}	1.663	3.259	5.198	8.229	13.56	22.44

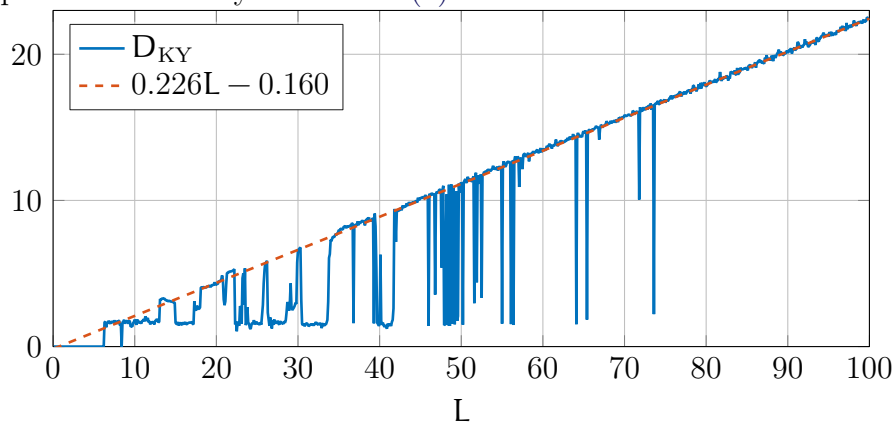
straightforwardly estimate the j for which $\sum_{i=1}^j \lambda_i \approx 0$, namely $j \approx 0.2L - 0.2$. This is acceptably close to the Kaplan–Yorke dimension $D_{KY} \approx 0.226L - 0.160$ shown in Figure 8 and obtained from extensive computation.

Table 1 presents Lyapunov exponents and Kaplan–Yorke dimensions for six different periodic domain sizes $L = 12, 13.5, 22, 36, 60, 100$,¹ whereas Table 2 presents Lyapunov exponents and Kaplan–Yorke dimensions for six different odd-periodic domain sizes $L = 17.5, 18.1, 18.2, 41, 60, 100$. These tables demonstrate how the increasingly positive Lyapunov exponents reveal the onset of chaotic dynamics and the increasing dimension of the chaotic attractor. These calculations of the Lyapunov exponents and Kaplan–Yorke dimensions with odd periodic domains are compatible with previously calculated Kaplan–Yorke dimensions (Rempel et al. 2004).

Figure 8 shows that as the domain size L increases, the Kaplan–Yorke dimension scales linearly with $D_{KY} \propto 0.226L$ for sufficiently large L ($L \gtrsim 80$). Similarly, in the case of rigid boundary conditions $\mathbf{u}, \partial_x \mathbf{u} = 0$ at $x = 0$ and at $x = L$ both Manneville (1985) and Tajima and Greenside (2002) found the Kaplan–Yorke dimension to scale as $0.230L$ when $50 < L < 400$. The small 2% difference in the coefficient suggests that the scaling of the Kaplan–Yorke

¹The case $L = 22$ is chosen for comparison with the Lyapunov exponents of Cvitanović, Davidchack, and Siminos (2010): our Lyapunov exponents agree with theirs to a difference of about 0.002.

- periodic boundary conditions (2)



- odd-periodic (3)

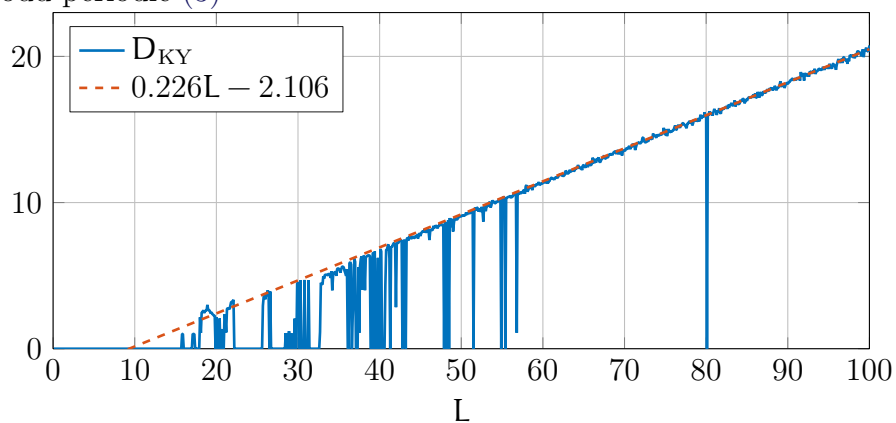


Figure 8: The Kaplan–Yorke dimension D_{KY} dependence on domain size L , computed for the Kuramoto–Sivashinsky PDE (1) on the (top) periodic spatial domain (2), and (bottom) odd-periodic spatial domain (3). In both cases, the Kaplan–Yorke dimension increases linearly with the domain size L , with $D_{KY} \approx 0.226L - c$ for $c = 0.160$ and 2.106 , respectively. This linearity appears most accurate for larger domains, $L \gtrsim 80$. At lower domain sizes, $L \lesssim 80$, there are several non-chaotic regions where the Kaplan–Yorke dimension is not of interest.

Table 2: the 12 most positive Lyapunov exponents and the Kaplan–Yorke dimension for several domain sizes L and odd-periodic boundary conditions (3).

	$L = 17.5$	$L = 18.1$	$L = 18.2$	$L = 41$	$L = 60$	$L = 100$
λ_1	-0.001	0.000	0.036	0.067	0.076	0.094
λ_2	-0.166	-0.003	-0.001	0.038	0.056	0.077
λ_3	-0.272	-0.194	-0.073	0.017	0.042	0.063
λ_4	-0.299	-0.280	-0.268	0.001	0.027	0.056
λ_5	-0.300	-0.377	-0.359	-0.008	0.021	0.044
λ_6	-0.526	-4.813	-4.044	-0.029	0.006	0.036
λ_7	-0.619	-4.923	-4.348	-0.076	0.000	0.031
λ_8	-1.794	-1.391	-1.395	-0.162	-0.007	0.022
λ_9	-3.780	-3.145	-3.070	-0.237	-0.029	0.017
λ_{10}	-6.513	-5.525	-5.383	-0.283	-0.050	0.008
λ_{11}	-9.692	-8.700	-8.538	-0.318	-0.094	0.001
λ_{12}	-9.854	-9.540	-10.10	-0.355	-0.146	0.000
D_{KY}	0.000	1.081	2.482	7.056	11.35	20.75

dimension for the Kuramoto–Sivashinsky PDE (1) on domain sizes $L \gtrsim 80$ only depends on the nature of the given boundary condition through an additive constant. In contrast, for smaller domain sizes $L \lesssim 50$, all points in the domain are somewhat close to a boundary and boundary effects play a more dominant role in the dynamics. The linear scaling of the attractor, here measured with the Kaplan–Yorke dimension, is a defining feature of an extensively chaotic system (e.g., Cross and Hohenberg 1993; Greenside 1996).

5 Conclusion

Through an exhaustive computation and analysis of the positive and least negative Lyapunov exponents, we investigated the development of spatio-temporal chaos in the Kuramoto–Sivashinsky PDE (1) as the domain size L increases. We found new details about how the Lyapunov exponents and the Kaplan–Yorke dimension increase with domain size, and are able to identify successive transitions into more chaotic regimes as individual Lyapunov exponents change sign from negative to positive, indicating additional directions in which trajectories of the chaotic system diverge.

The spatial extensivity of the Kuramoto–Sivashinsky PDE (1) that we have confirmed here in new detail indicates that the system in a large domain may

be viewed as composed of interacting subsystems, approximately uncorrelated for short enough times (e.g., Wittenberg and Holmes 1999; Yang et al. 2009; Greenside 1996). This interpretation suggests that we should be able to successfully simulate the ‘turbulence’ in the Kuramoto–Sivashinsky PDE (1) on very large domains by appropriately coupling relatively small patches of simulations across space using the equation-free paradigm (e.g., Kevrekidis and Samaey 2009). Exactly what may be appropriate coupling is the subject of ongoing research.

Acknowledgements This research was partly supported by the research grant DP150102385 from the Australian Research Council, and RAE was financially supported by the Australian Government Research Training Program.

References

- Benettin, G., L. Galgani, A. Giorgilli, and J.-M. Strelcyn (1980a). “Lyapunov Characteristic Exponents for smooth dynamical systems and for hamiltonian systems; A method for computing all of them. Part 2: Numerical application”. In: *Meccanica* 15.1, pp. 21–30. DOI: [10.1007/BF02128237](https://doi.org/10.1007/BF02128237). (Cit. on pp. 2, 8).
- (1980b). “Lyapunov Characteristic Exponents for smooth dynamical systems and for hamiltonian systems; A method for computing all of them. Part 2: Numerical application”. In: *Meccanica* 15.1, pp. 21–30. DOI: [10.1007/BF02128237](https://doi.org/10.1007/BF02128237). (Cit. on pp. 7, 8).
- Chertovskih, R., E. V. Chimanski, and E. L. Rempel (2015). “Route to hyperchaos in Rayleigh–Bénard convection”. In: *EPL (Europhysics Letters)* 112.1, p. 14001. DOI: [10.1209/0295-5075/112/14001](https://doi.org/10.1209/0295-5075/112/14001). (Cit. on p. 2).
- Chicone, C. (2006). *Ordinary Differential Equations with Applications*. Vol. 34. Texts in Applied Mathematics. Springer, New York, NY. DOI: [10.1007/0-387-35794-7](https://doi.org/10.1007/0-387-35794-7) (cit. on p. 7).
- Cross, M. C. and P. C. Hohenberg (1993). “Pattern formation outside of equilibrium”. In: *Rev. Mod. Phys.* 65, pp. 851–1112. DOI: [10.1103/RevModPhys.65.851](https://doi.org/10.1103/RevModPhys.65.851). (Cit. on pp. 2, 4, 17).
- Cvitanović, P., R. Davidchack, and E. Siminos (2010). “On the state space geometry of the Kuramoto–Sivashinsky flow in a periodic domain”. In: *SIAM J. Appl. Dyn. Syst.* 9.1, pp. 1–33. DOI: [10.1137/070705623](https://doi.org/10.1137/070705623). (Cit. on pp. 2, 4, 15).

- Dankowicz, H., P. Holmes, G. Berkooz, and J. Elezgaray (1996). “Local models of spatio-temporally complex fields”. In: *Physica D* 90.4, pp. 387–407. DOI: [10.1016/0167-2789\(95\)00245-6](https://doi.org/10.1016/0167-2789(95)00245-6). (Cit. on pp. 2, 4).
- Dieci, L., R. Russell, and E. Van Vleck (1997). “On the Computation of Lyapunov Exponents for Continuous Dynamical Systems”. In: *SIAM J. Numer. Anal.* 34.1, pp. 402–423. DOI: [10.1137/S0036142993247311](https://doi.org/10.1137/S0036142993247311). (Cit. on pp. 7, 8).
- Eckmann, J.-P. and D. Ruelle (1985). “Ergodic theory of chaos and strange attractors”. In: *Rev. Mod. Phys.* 57, pp. 617–656. DOI: [10.1103/RevModPhys.57.617](https://doi.org/10.1103/RevModPhys.57.617). (Cit. on pp. 2, 7).
- Eguíluz, V. M., P. Alstrøm, E. Hernández-García, and O. Piro (1999). “Average patterns of spatiotemporal chaos: A boundary effect”. In: *Phys. Rev. E* 59, pp. 2822–2825. DOI: [10.1103/PhysRevE.59.2822](https://doi.org/10.1103/PhysRevE.59.2822). (Cit. on p. 4).
- Foias, C., B. Nicolaenko, G. R. Sell, and R. Temam (1986). *Inertial manifolds for the Kuramoto–Sivashinsky equation and an estimate of their lowest dimension*. Technical report, University of Minnesota Digital Conservancy. URL: <http://hdl.handle.net/11299/4494> (cit. on p. 4).
- Geist, K., U. Parlitz, and W. Lauterborn (1990). “Comparison of Different Methods for Computing Lyapunov Exponents”. In: *Prog. Theor. Phys.* 83.5, pp. 875–893. DOI: [10.1143/PTP.83.875](https://doi.org/10.1143/PTP.83.875). (Cit. on pp. 7, 8).
- Grassberger, P. and I. Procaccia (1983). “Measuring the strangeness of strange attractors”. In: *Physica D* 9.1, pp. 189–208. DOI: [10.1016/0167-2789\(83\)90298-1](https://doi.org/10.1016/0167-2789(83)90298-1). (Cit. on pp. 3, 14).
- Greenside, H. S. (1996). *Spatiotemporal Chaos in Large Systems: The Scaling of Complexity with Size*. Technical report. URL: <https://arxiv.org/abs/chao-dyn/9612004> (cit. on pp. 17, 18).
- Hassanally, M. and V. Raman (2018). “Ensemble-LES analysis of perturbation response of turbulent partially-premixed flames”. In: *Proceedings of the Combustion Institute*. DOI: [10.1016/j.proci.2018.06.209](https://doi.org/10.1016/j.proci.2018.06.209) (cit. on p. 2).
- Hohenberg, P. C. and B. I. Shraiman (1989). “Chaotic behavior of an extended system”. In: *Physica D* 37.1, pp. 109–115. DOI: [10.1016/0167-2789\(89\)90121-8](https://doi.org/10.1016/0167-2789(89)90121-8). (Cit. on p. 2).
- Hyman, J. M. and B. Nicolaenko (1986). “The Kuramoto–Sivashinsky equation: A bridge between PDEs and dynamical systems”. In: *Physica D* 18.1, pp. 113–126. DOI: [10.1016/0167-2789\(86\)90166-1](https://doi.org/10.1016/0167-2789(86)90166-1). (Cit. on pp. 2, 4).
- Kaplan, J. L. and J. A. Yorke (1979). “Chaotic behavior of multidimensional difference equations”. In: *Functional Differential Equations and*

- Approximation of Fixed Points*. Ed. by H.-O. Peitgen and H.-O. Walther. Springer, Berlin Heidelberg, pp. 204–227 (cit. on pp. 3, 14).
- Keefe, L., P. Moin, and J. Kim (1992). “The dimension of attractors underlying periodic turbulent Poiseuille flow”. In: *Journal of Fluid Mechanics* 242, pp. 1–29. DOI: [10.1017/S0022112092002258](https://doi.org/10.1017/S0022112092002258) (cit. on p. 2).
- Kevrekidis, I. G. and G. Samaey (2009). “Equation-Free Multiscale Computation: Algorithms and Applications”. In: *Annu. Rev. Phys. Chem.* 60, pp. 321–44. DOI: [10.1146/annurev.physchem.59.032607.093610](https://doi.org/10.1146/annurev.physchem.59.032607.093610) (cit. on p. 18).
- Kuramoto, Y. and T. Tsuzuki (1976). “Persistent Propagation of Concentration Waves in Dissipative Media Far from Thermal Equilibrium”. In: *Prog. Theor. Phys.* 55.2, pp. 356–369. DOI: [10.1143/PTP.55.356](https://doi.org/10.1143/PTP.55.356). (Cit. on p. 2).
- Lan, Y. and P. Cvitanović (2008). “Unstable recurrent patterns in Kuramoto-Sivashinsky dynamics”. In: *Phys. Rev. E* 78, p. 026208. DOI: [10.1103/PhysRevE.78.026208](https://doi.org/10.1103/PhysRevE.78.026208). (Cit. on p. 4).
- Manneville, P. (1985). “Liapounov exponents for the Kuramoto–Sivashinsky model”. In: *Macroscopic Modelling of Turbulent Flows*. Ed. by U. Frisch, J. B. Keller, G. C. Papanicolaou, and O. Pironneau. Springer, Berlin Heidelberg, pp. 319–326 (cit. on pp. 3, 9, 15).
- Pomeau, Y. and S. Zaleski (1985). “The Kuramoto–Sivashinsky equation: A caricature of hydrodynamic turbulence?” In: *Macroscopic Modelling of Turbulent Flows*. Ed. by U. Frisch, J. B. Keller, G. C. Papanicolaou, and O. Pironneau. Springer, Berlin Heidelberg, pp. 296–303 (cit. on p. 2).
- Rempel, E. L., A. C.-L. Chian, E. E. N. Macau, and R. R. Rosa (2004). “Analysis of chaotic saddles in high-dimensional dynamical systems: The Kuramoto–Sivashinsky equation”. In: *Chaos* 14.3, pp. 545–556. DOI: [10.1063/1.1759297](https://doi.org/10.1063/1.1759297). (Cit. on pp. 4, 15).
- Ruelle, D. (1979). “Ergodic theory of differentiable dynamical systems”. In: *Publications mathématiques de l’IHÉS* 50.1, pp. 27–58. DOI: [10.1007/bf02684768](https://doi.org/10.1007/bf02684768) (cit. on p. 7).
- Ruelle, D. and F. Takens (1971). “On the nature of turbulence”. In: *Communications in Mathematical Physics* 20.3, pp. 167–192. DOI: [10.1007/BF01646553](https://doi.org/10.1007/BF01646553) (cit. on p. 2).
- Shimada, I. and T. Nagashima (1979). “A Numerical Approach to Ergodic Problem of Dissipative Dynamical Systems”. In: *Prog. Theor. Phys.* 61.6, pp. 1605–1616. DOI: [10.1143/PTP.61.1605](https://doi.org/10.1143/PTP.61.1605). (Cit. on pp. 2, 7, 8).
- Sivashinsky, G. I. (1977). “Nonlinear analysis of hydrodynamic instability in laminar flames—I. Derivation of basic equations”. In: *Acta Astronautica* 4.11, pp. 1177–1206. DOI: [10.1016/0094-5765\(77\)90096-0](https://doi.org/10.1016/0094-5765(77)90096-0). (Cit. on p. 2).

- Sivashinsky, G. I. and D. M. Michelson (1980). “On Irregular Wavy Flow of a Liquid Film Down a Vertical Plane”. In: *Progress of Theoretical Physics* 63.6, pp. 2112–2114. DOI: [10.1143/PTP.63.2112](https://doi.org/10.1143/PTP.63.2112). (Cit. on p. 2).
- Skokos, C. (2010). “The Lyapunov Characteristic Exponents and Their Computation”. In: *Dynamics of Small Solar System Bodies and Exoplanets*. Ed. by J. J. Souchay and R. Dvorak. Springer, Berlin Heidelberg, pp. 63–135. DOI: [10.1007/978-3-642-04458-8_2](https://doi.org/10.1007/978-3-642-04458-8_2). (Cit. on pp. 7, 8).
- Sprott, J. C. (2010). *Elegant chaos: Algebraically simple chaotic flows*. World Scientific, Singapore. DOI: [10.1142/7183](https://doi.org/10.1142/7183) (cit. on pp. 2, 4).
- Tajima, S. and H. S. Greenside (2002). “Microextensive chaos of a spatially extended system”. In: *Phys. Rev. E* 66, p. 017205. DOI: [10.1103/PhysRevE.66.017205](https://doi.org/10.1103/PhysRevE.66.017205). (Cit. on pp. 2, 3, 15).
- Takens, F. (1981). “Detecting strange attractors in turbulence”. In: *Lecture Notes in Mathematics*. Berlin, Heidelberg: Springer Berlin Heidelberg, pp. 366–381. DOI: [10.1007/bfb0091924](https://doi.org/10.1007/bfb0091924) (cit. on p. 2).
- Wittenberg, R. W. and P. Holmes (1999). “Scale and space localization in the Kuramoto–Sivashinsky equation”. In: *Chaos* 9.2, pp. 452–465. DOI: [10.1063/1.166419](https://doi.org/10.1063/1.166419). (Cit. on pp. 4, 9, 18).
- Xu, M. (2017). “Spatiotemporal Chaos in Large Systems Driven Far-From-Equilibrium: Connecting Theory with Experiment”. PhD thesis. Virginia Polytechnic Institute and State University. URL: <https://vtechworks.lib.vt.edu/handle/10919/79499> (cit. on p. 2).
- Yang, H.-L., K. A. Takeuchi, F. Ginelli, H. Chaté, and G. Radons (2009). “Hyperbolicity and the effective dimension of spatially extended dissipative systems”. In: *Phys. Rev. Lett.* 102, p. 074102. DOI: [10.1103/PhysRevLett.102.074102](https://doi.org/10.1103/PhysRevLett.102.074102). (Cit. on pp. 9, 18).